

Highlightable Ca²⁺ Indicators for Live Cell Imaging

Hiofan Hoi,[†] Tomoki Matsuda,[‡] Takeharu Nagai,[‡] and Robert E. Campbell^{*,†}

[†]Department of Chemistry, University of Alberta, Edmonton, Alberta, Canada T6G 2G2

[‡]The Institute of Scientific and Industrial Research, Osaka University, Mihogaoka 8-1, Ibaraki, Osaka 567-0047, Japan

S Supporting Information

ABSTRACT: Two of the most powerful implementations of fluorescent protein (FP) technology are “highlighters”, which can be converted from nonfluorescent to fluorescent or from one color to another by illumination, and calcium ion (Ca²⁺) indicators. Combining the properties of both of these FP classes into a single construct would produce a highlightable Ca²⁺ indicator that would enable researchers to mark a single cell spectrally in a transfected tissue and image its intracellular Ca²⁺ dynamics. In an effort to create such a hybrid tool, we explored three different protein design strategies. The strategy that ultimately proved successful involved the creation of a circularly permuted version of a green-to-red photoconvertible FP and its introduction into a G-CaMP-type single-FP-based Ca²⁺ indicator. Optimization by directed evolution led to the identification of two promising variants that exhibit excellent photoconversion properties and have an up to 4.6-fold increase in red fluorescence intensity upon binding of Ca²⁺. We demonstrate the utility of these variants in HeLa cells and rat hippocampal neurons.

The calcium ion (Ca²⁺) is one of the most important second messengers in cell signaling pathways. It plays key roles in numerous cellular processes such as fertilization, development, and learning and memory.¹ Over the past several decades, a wide range of tools have been developed to monitor Ca²⁺ dynamics in live cells, tissues, or whole animals. The current arsenal of Ca²⁺ indicators includes designs based on both synthetic organic dyes and engineered fluorescent proteins (FPs).² As FP-based Ca²⁺ indicators are genetically encodable, they can be introduced into cells using the minimally invasive method of plasmid DNA transfection. Relative to synthetic dyes, FP-based indicators have the additional advantages of targeting to subcellular compartments and expression in transgenic organisms.³

While the current toolbox of Ca²⁺ indicators provides a variety of choices with respect to indicator class (genetic vs synthetic), fluorescence hue, and Ca²⁺ affinity, there is a continued demand for new tools with improved or unprecedented properties.^{2,4} One desirable property of a Ca²⁺ indicator would be the ability to highlight specific experimenter-chosen cells within a tissue to allow their Ca²⁺ dynamics to be imaged in a distinct spectral channel. This would enable researchers to isolate spectrally and image the activity of specific cells in a transgenic animal with ubiquitous expression of a suitable genetically encoded indicator. Similarly, irreversible

highlighting would allow researchers to return to and image the activity of a cell imaged in an earlier experiment.

In an effort to create a highlightable Ca²⁺ indicator for live cell imaging, we attempted to use protein engineering to combine the properties of a well-established class of FP-based Ca²⁺ indicators with the properties of three previously reported classes of photoactivatable (pa) or photoconvertible (pc) FPs. The class of FP-based Ca²⁺ indicators used in this work is the single FP design common to the Pericam and G-CaMP series of indicators.^{5–8} In this design, the calcium-binding protein calmodulin (CaM) and its binding peptide M13 (from skeletal muscle myosin light-chain kinase) are genetically fused to the N- and C- termini of a circularly permuted FP (cpFP). Conformational changes resulting from binding of Ca²⁺ by CaM lead to a change in the FP chromophore environment that increases its fluorescence.^{9,10} Our lab has recently reported a method for high-throughput screening of large libraries of G-CaMP variants for identification of mutants with improved function or altered fluorescence hue.¹¹ This effort produced the GECO series of multicolored Ca²⁺ indicators that served as the templates for this work.

The three classes of paFPs and pcFPs explored in this work were (1) the paGFP type, whose green fluorescence increases upon illumination with violet (~400 nm) light;¹² (2) the pamCherry type, whose red fluorescence increases upon illumination with violet light;¹³ and (3) the Kaede type, which irreversibly converts from green- to red-fluorescent upon illumination with violet light (Figure 1).¹⁴ We reasoned that introducing the key mutations responsible for these pa or pc

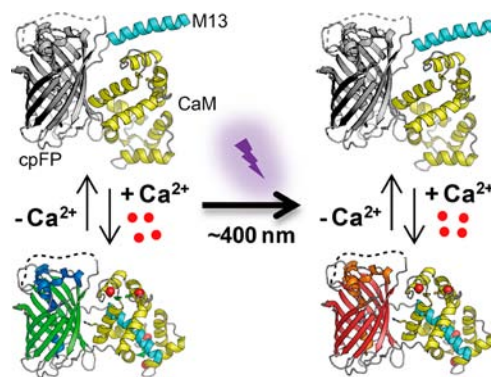


Figure 1. Schematic representation of a single-FP-based green-to-red photoconvertible Ca²⁺ indicator.

Received: October 15, 2012

Published: December 20, 2012

phenotypes into the FP module of appropriate GECOs could produce pa- or pcGECOs. We initially tested this hypothesis by introducing the substitutions responsible for the photoactivation property of paGFP into green-emissive GECOs, including G-GECO1.1–1.3, GEM-GECO1, and GEX-GECO1.¹¹ We found that all of the resulting variants had severely diminished responses to Ca^{2+} and no photoactivation after prolonged illumination at 405 nm in *Escherichia coli* colonies. In a parallel effort, we attempted to convert R-GECO1, in which the FP portion is a close homologue of the *Discosoma*-derived pamCherry,¹¹ into a paGECO. Although we did identify several variants that underwent photoactivation upon violet-light irradiation, their Ca^{2+} responses were disappointingly small ($\Delta F/F_{\text{min}} = 15\text{--}30\%$) (Figure S1). Further discussion of these unsuccessful efforts is provided in the Supporting Information.

We next turned to Kaede-type pcFPs, for which there exist no GECO variants with high sequence homology. Accordingly, we undertook a complete swap of the cpFP portion of G-GECO1.1 with a cp version of a Kaede-type pcFP known as mMaple.¹⁵ We first created a series of cpmMaple variants with the original termini connected by a $(\text{Gly})_2\text{Ser}(\text{Gly})_2$ linker and new termini at residues 140, 145, 193, and 207. Not unexpectedly, we found that variants with new termini far from the chromophore at interstrand loops (i.e., 193 and 207) retained the photoconversion property and much of the brightness of mMaple (Figure S2 and Table S1). In contrast, cp variants with new termini near the chromophore in β -strand 7 (i.e., 140 and 145) were substantially dimmer though still photoconvertible. Since the variant with new termini at position 145 was the closest analogue of the cpFP portion of other single-FP-based Ca^{2+} indicators, we introduced it in place of the cpFP of G-GECO1.1 despite its low brightness. Satisfyingly, we found that the resulting construct was weakly fluorescent but capable of green-to-red photoconversion. It also displayed a small increase in red fluorescence upon Ca^{2+} binding ($\sim 20\%$). We named this first generation pcGECO as green-to-red (GR)-GECO0.1 and used it as the initial template for an extensive process of optimization for improved brightness and Ca^{2+} response in the red channel.

Initial efforts to optimize the response of GR-GECO focused on exploring different lengths and compositions of the peptide sequences linking the cpFP domain to CaM and M13 (Table S2). These and all subsequent libraries were screened in *E. coli* colonies using our previously reported periplasmic export strategy combined with on-plate photoactivation using a custom-built 405 nm LED illumination chamber and fluorescence image-based screening.^{11,16} This effort ultimately led to the identification of GR-GECO0.2 with two additional residues (Gly-Tyr) in the linker between M13 and the cpFP domain. We next turned our attention to the presumed interface between the cpFP domain and the CaM/M13 complex. X-ray crystallographic analysis of G-CaMP2 plus various mutagenesis studies have identified a number of residues (e.g., Glu61, Arg377, Asn380, and Asp381; G-CaMP2 numbering) that are in this interface and help to communicate the Ca^{2+} -dependent conformational change into a change in the FP chromophore environment.^{9,10} Libraries of GR-GECO variants created by genetic randomization of these positions were screened for improved efficiency of photoconversion and improved Ca^{2+} response for the red species. This effort led to the identification of GR-GECO0.3 with three additional substitutions (E61P/N380W/D381G), which ex-

hibited improved brightness, photoconversion, and response to Ca^{2+} ($\sim 100\%$) relative to GR-GECO0.2 (Table S3). Subsequently, we resorted to the use of directed evolution through iterative rounds of library creation by error-prone PCR and library screening for improved photoconversion efficiency and increased Ca^{2+} response of the red species. After 16 rounds, we arrived at five variants that showed satisfying photoconversion and Ca^{2+} response. On the basis of an assessment of both in vitro properties and performance in live cell imaging, we selected two variants, designated as GR-GECO1.1 and GR-GECO1.2, as the most preferred final versions. GR-GECO1.1 displays satisfying Ca^{2+} response by both the green and red species, whereas GR-GECO1.2 exhibits excellent Ca^{2+} response by the red species (Table S4). GR-GECO1.1 has 28 mutations or insertions distributed around the protein, while GR-GECO1.2 has 24 mutations or insertions (Figures S3 and S4 and Table S3).

Spectroscopic characterization of the purified proteins revealed that the green and red states of GR-GECO1.1 exhibit 8.6- and 6.1-fold increases in fluorescence, respectively, upon binding of Ca^{2+} , while GR-GECO1.2 exhibits 3.9- and 6.7-fold increases, respectively (Figure 2). The absorbance spectra of

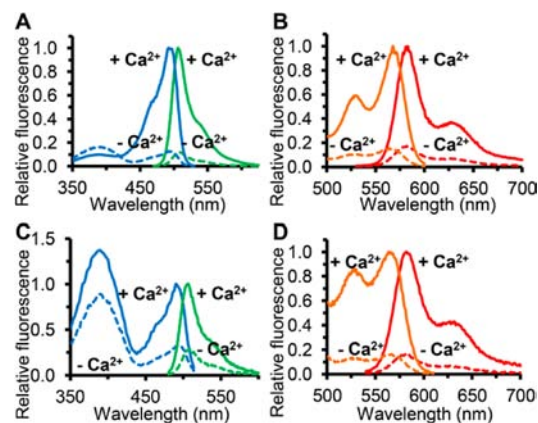


Figure 2. Excitation and emission spectra of the (A, C) green and (B, D) red forms of (A, B) GR-GECO1.1 and (C, D) GR-GECO1.2 in the presence (solid curves) or absence (dashed curves) of Ca^{2+} .

both GR-GECOs revealed that in the absence of Ca^{2+} , both the green- and red-state chromophores exist predominantly in their nonfluorescent protonated forms at pH 7.4 (Figure S5). Binding of Ca^{2+} shifts the chromophores into their fluorescent anionic states. Accordingly, the GR-GECOs share a Ca^{2+} sensing mechanism similar to that of G-CaMPs and G-GECOs. As observed for the GECO variants,¹¹ the Ca^{2+} sensing mechanism is best described as a Ca^{2+} -dependent shift in the chromophore pK_a to a lower value, with larger shifts giving rise to larger fluorescence responses.

In vitro Ca^{2+} titrations enabled us to determine the values of K'_d (defined as the concentration of Ca^{2+} that gives half the maximum fluorescence increase) for GR-GECO1.1 (86 and 54 nM for the green and red species, respectively) and GR-GECO1.2 (74 and 90 nM, respectively) (Figure S6 and Table S4). Further characterization by stopped-flow fluorescence spectroscopy demonstrated that the relaxation rate profiles of GR-GECO1.1 at different Ca^{2+} concentrations followed monoexponentially increasing functions and give Hill coefficients and K'_d values consistent with those obtained by Ca^{2+} titration (Figure S7 and Table S5). In contrast, GR-GECO1.2

exhibited complex stopped-flow kinetics, and the data could not be satisfactorily fit to a simple kinetic model (Figure S7).

Since reversible photoswitching between the protonated and deprotonated states of red species has been observed with mEos2 and mMaple,^{15,17} we examined the GR-GECOs for such behavior. Fortunately, prolonged illumination of the protonated state ($\lambda_{\text{max}} = 455 \text{ nm}$) did not reversibly shift the equilibrium toward the deprotonated state in either the presence or the absence of Ca^{2+} (Figure S8). However, we did notice that excitation of the protonated state of the green species of GR-GECO1.2 ($\lambda_{\text{max}} = 383 \text{ nm}$) resulted in significant green emission (Figure 2). In contrast, mMaple exhibits negligible green fluorescence when excited at this absorbance peak. We reasoned that this green emission is likely the result of excited-state proton transfer (ESPT),¹⁸ which must compete with the photoconversion process. In agreement with this hypothesis, we observed slower photoconversion in GR-GECO1.2 than in GR-GECO1.1 (Figure S9).

To determine how GR-GECOs would perform in live cell imaging, we expressed them in HeLa cells and, following partial photoconversion by illumination of the whole field of view with violet light, used established protocols to determine their response to changes in cytoplasmic Ca^{2+} concentrations.⁴ As expected, we observed oscillations, decreases to minima, and increases to maxima in the fluorescence intensity when cells were treated with histamine, EGTA/ionomycin, and Ca^{2+} /ionomycin, respectively (Figure 3). In cells, the dynamic ranges for the green and red species, respectively, were 9.4- and 3.4-fold for GR-GECO1.1 and 6.2- and 5.1-fold for GR-GECO1.2 (Table S4).

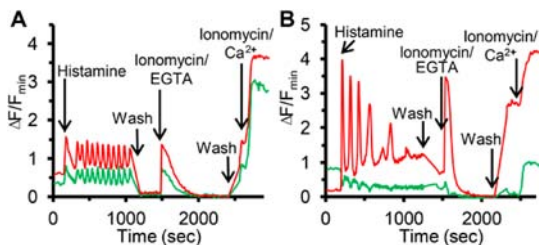


Figure 3. Representative time-course traces for HeLa cells expressing cytoplasmic (A) GR-GECO1.1 or (B) GR-GECO1.2. For GR-GECO1.2, the red species displayed a larger dynamic range and greater photostability than the green species.

To demonstrate the primary advantage of a highlightable Ca^{2+} indicator, we used light from a 405 nm laser to highlight single cells in a population of GR-GECO1.1-expressing HeLa cells (Figures S10, S11 and S12 and Movie S1). As expected, only the highlighted cells were observed in the red emission channel, and they exhibited typical histamine-induced Ca^{2+} oscillations. Similarly, we found that single cells in a population of primary neurons transfected with GR-GECO1.2 could be highlighted and spontaneous Ca^{2+} oscillations could be imaged in the red emission channel (Figure 4 and Movie S2). We anticipate that highlightable Ca^{2+} indicators will facilitate the dissection and study of Ca^{2+} signaling in neuronal networks.

In conclusion, we have engineered, characterized, and validated photoconvertible Ca^{2+} indicators for live cell fluorescence imaging. By enabling the selective highlighting and imaging of individual cells in densely transfected tissues, these indicators will enable researchers to explore intra- and

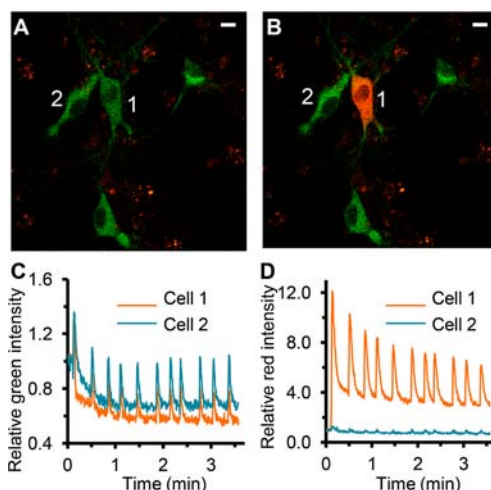


Figure 4. GR-GECO1.2 expressed in dissociated hippocampal neurons. (A, B) Merged green and red fluorescence images of cells (A) before and (B) after photoactivation of cell 1. Images were taken from Movie S2. Scale bar $10 \mu\text{m}$. (C, D) Imaging of spontaneous Ca^{2+} oscillations in the (C) green and (D) red emission channels.

intercellular signaling with unprecedented experimental control and versatility.

■ ASSOCIATED CONTENT

📄 Supporting Information

Additional discussion of unsuccessful pa/pcGECO designs, Materials and Methods, figures and tables for additional protein characterization, primer list, and movies (AVI). This material is available free of charge via the Internet at <http://pubs.acs.org>.

■ AUTHOR INFORMATION

Corresponding Author

robert.e.campbell@ualberta.ca

Notes

mMaple, the template for construction of the GR-GECOs, is covered by an US patent application jointly owned by the University of Alberta and Allele Biotechnology.

■ ACKNOWLEDGMENTS

We thank the University of Alberta MBSU, INRF, Yongxin Zhao, Andy Holt, and Christopher W. Cairo for support and technical assistance. Funding support was provided by NSERC. R.E.C. holds a Tier II Canada Research Chair. Grant-in-Aid for Scientific Research on Innovative Areas from MEXT (23115003) and FIRST from JSPS (T.N.).

■ REFERENCES

- (1) Berridge, M. J.; Lipp, P.; Bootman, M. D. *Nat. Rev. Mol. Cell Biol.* **2000**, *1*, 11.
- (2) Grienberger, C.; Konnerth, A. *Neuron* **2012**, *73*, 862.
- (3) Kotlikoff, M. I. *J. Physiol.* **2007**, *578*, 55.
- (4) Palmer, A. E.; Giacomello, M.; Kortemme, T.; Hires, S. A.; Lev-Ram, V.; Baker, D.; Tsien, R. Y. *Chem. Biol.* **2006**, *13*, 521.
- (5) Nagai, T.; Sawano, A.; Park, E. S.; Miyawaki, A. *Proc. Natl. Acad. Sci. U.S.A.* **2001**, *98*, 3197.
- (6) Nakai, J.; Ohkura, M.; Imoto, K. *Nat. Biotechnol.* **2001**, *19*, 137.
- (7) Tallini, Y. N.; Ohkura, M.; Choi, B. R.; Ji, G.; Imoto, K.; Doran, R.; Lee, J.; Plan, P.; Wilson, J.; Xin, H. B.; Sanbe, A.; Gulick, J.; Mathai, J.; Robbins, J.; Salama, G.; Nakai, J.; Kotlikoff, M. I. *Proc. Natl. Acad. Sci. U.S.A.* **2006**, *103*, 4753.

(8) Tian, L.; Hires, S. A.; Mao, T.; Huber, D.; Chiappe, M. E.; Chalasani, S. H.; Petreanu, L.; Akerboom, J.; McKinney, S. A.; Schreiter, E. R.; Bargmann, C. I.; Jayaraman, V.; Svoboda, K.; Looger, L. L. *Nat. Methods* **2009**, *6*, 875.

(9) Wang, W.; Fang, H.; Groom, L.; Cheng, A.; Zhang, W.; Liu, J.; Wang, X.; Li, K.; Han, P.; Zheng, M.; Yin, J.; Wang, W.; Mattson, M. P.; Kao, J. P.; Lakatta, E. G.; Sheu, S. S.; Ouyang, K.; Chen, J.; Dirksen, R. T.; Cheng, H. *Cell* **2008**, *134*, 279.

(10) Akerboom, J.; Rivera, J. D.; Guilbe, M. M.; Malavé, E. C.; Hernandez, H. H.; Tian, L.; Hires, S. A.; Marvin, J. S.; Looger, L. L.; Schreiter, E. R. *J. Biol. Chem.* **2009**, *284*, 6455.

(11) Zhao, Y.; Araki, S.; Wu, J.; Teramoto, T.; Chang, Y. F.; Nakano, M.; Abdelfattah, A. S.; Fujiwara, M.; Ishihara, T.; Nagai, T.; Campbell, R. E. *Science* **2011**, *333*, 1888.

(12) Patterson, G. H.; Lippincott-Schwartz, J. *Science* **2002**, *297*, 1873.

(13) Subach, F. V.; Patterson, G. H.; Manley, S.; Gillette, J. M.; Lippincott-Schwartz, J.; Verkhusha, V. V. *Nat. Methods* **2009**, *6*, 153.

(14) Ando, R.; Hama, H.; Yamamoto-Hino, M.; Mizuno, H.; Miyawaki, A. *Proc. Natl. Acad. Sci. U.S.A.* **2002**, *99*, 12651.

(15) McEvoy, A. L.; Hoi, H.; Bates, M.; Platonova, E.; Cranfill, P. J.; Davidson, M. W.; Ewers, H.; Liphardt, J.; Campbell, R. E. *PLoS One* **2012**, *7*, No. e51314.

(16) Hoi, H.; Shaner, N. C.; Davidson, M. W.; Cairo, C. W.; Wang, J.; Campbell, R. E. *J. Mol. Biol.* **2010**, *401*, 776.

(17) Annibale, P.; Scarselli, M.; Kodyan, A.; Radenovic, A. *J. Phys. Chem. Lett.* **2010**, *1*, 1506.

(18) Chattoraj, M.; King, B. A.; Bublitz, G. U.; Boxer, S. G. *Proc. Natl. Acad. Sci. U.S.A.* **1996**, *93*, 8362.